Consistent generation of ice-streams via thermo-viscous instabilities modulated by membrane stresses

Richard C. A. Hindmarsh[1]

Received 2 December 2008; revised 13 February 2009; accepted 24 February 2009; published 25 March 2009.

[1] Accurate computation of ice-stream location and dynamics is a key aspiration for theoretical glaciology. Ice-sheet models with thermo-viscous coupling have been shown to exhibit stream-like instabilities using shallow-ice approximation mechanics, but the location and width of these streams depends on the numerical implementation and are not unique. We present results from thermo-viscously coupled ice-sheet models incorporating membrane stresses. Spontaneous generation of fast-flowing linear features still occurs under certain parameter regimes, with computed stream widths between 20 km to 100 km, comparable with observations. These features are maintained as the grid-size is decreased. The thermo-viscous feedback mechanism that generates ice-streams under the shallow ice approximation still operates, now selecting a unique stream size. Computations of thermo-viscous ice flows should include membrane stresses when the bed is approximately flat, e.g. parts of Antarctica and former ice-sheets of the Northern hemisphere. Previous calculations of spontaneous ice-stream generation using the shallow ice approximation should be reassessed. **Citation:** Hindmarsh, R. C. A. (2009), Consistent generation of ice-streams via thermo-viscous instabilities modulated by membrane stresses, *Geophys. Res. Lett.*, *36*, L06502, doi:10.1029/2008GL036877.

1. Introduction

[2] Ice streams are a conspicuous patterning in ice-sheets, both in the surface topography and the surface velocity [*Bamber et al.*, 2001]. Their significance is due to their discharging a very substantial proportion of the accumulation of an ice-sheet, and exhibiting flow variability that possibly extends in scale up to the very large surges that played major roles in operation of the climate system (e.g., Heinrich Events [*MacAyeal*, 1993]). Consequently, the successful computation of ice-stream location and flow is one of the key goals of theoretical glaciology. However, even computing ice-stream location has been problematical up to now, with different models under the same forcing predicting different stream geometries [*Payne et al.*, 2000]. We consider the use of a more complex mechanical model, and demonstrate that this step allows consistent prediction of ice stream location.

[3] While many ice-streams are clearly associated with topographic lows in the bedrock (e.g., Pine Island Glacier [*Vaughan et al.*, 2006]), evidence from former ice-sheets, in particular the existence of cross-cutting lineations [*Clark*, 1993] shows that basal topography is not the only control on ice-stream location. The existence of thermo-viscous instabilities [e.g., *Payne*, 1995] in plane flow and related "hydraulic runaway" mechanisms [e.g., *Sayag and Tziperman*, 2008] has led to the suggestion and numerical demonstration that ice-streams might be generated by a map-plane fingering instability caused by coupling of the ice flow and the thermal field [*Fowler and Johnson*, 1996; *Payne and Dongelmans*, 1997]. Using the shallow-ice approximation (SIA), the latter authors presented calculations generated by a time-dependent numerical model that solved the flow and heat equations with a temperature-dependent ice viscosity, showing that certain parameter combinations (principally surface temperature and accumulation rate) generated ice-stream-like features. They argued that a fingering mechanism operated such that if a warmer area propagated upstream locally, it would draw flow in which generated localized heating, leading to less viscous ice, increased speeds, drawdown and further channelling of ice - an ice-flux capture mechanism. However, an intercomparison experiment between models from ten different groups [*Payne et al.*, 2000] although exhibiting instabilities, failed to generate comparable patterning, with considerable variation in detail shown in particular at short wavelengths. This raised the issue of whether the computed stream generation was a numerical artefact.

[4] In an effort to answer this question, *Hindmarsh* [2004] examined the linearized instability of the shallow ice approximation (SIA) in thermo-viscous calculations, and showed that its use was ill-posed at short wavelengths. *Hindmarsh* [2006a] showed that using mechanical models which incorporated horizontal stress gradients damped instabilities at short wavelengths, removing the ill-posing. He also showed that use of the membrane stress approximation (MSA) (i.e., the three-dimensional version of the longitudinal stress approximation, which includes horizontal stress gradients) [*Blatter*, 1995; *MacAyeal*, 1989; *Hindmarsh*, 2006b] was as accurate as use of the full Stokes equations for this application. *Sayag and Tziperman* [2008] found similar results using a related but different mechanism for generating instabilities. Previous workers [e.g., *Hulbe and MacAyeal*, 1999; *Marshall and Clarke*, 1997] have used membrane-stress approximations in thermo-mechanically coupled calculations, but not to address the issue of spontaneous ice-stream genesis.

[5] Using the SIA, *Hindmarsh* [2006a] presented some finite-amplitude (i.e., fully non-linear) calculations which showed that the patterning of basal temperature depended strongly on the discretization method used, arguing that

[1]Physical Sciences Division, British Antarctic Survey, Cambridge, UK.

Copyright 2009 by the American Geophysical Union.
0094-8276/09/2008GL036877

this was a symptom of the ill-posedness of the SIA. *Bueler et al.* [2007] have argued against this, suggesting that the problem lay in flaws in the construction of the numerical schemes. Some support for this idea comes from the work of *Saito et al.* [2006], who found that the use of higher-order stress models did not improve calculations of streams.

[6] Solving a well-posed system is essential to the success of numerical methods, so if we are to accept the reasoning of *Hindmarsh* [2006a], the implication is that incorporating horizontal stress gradients in thermo-mechanically coupled computations of ice-sheet evolution should produce results which, in the broad patterning at least, are independent of the grid-size and discretization method used. This paper examines this issue, adopting the simplest possible MSA due to *MacAyeal* [1989]. A set of parameters which generate steady streams using the SIA are used, and results are shown to depend on the grid-size used under conditions of grid refinement. The same set of parameters are then used to generate instabilities with the MSA, and here the results do not depend substantially on the grid used; moreover, the streams are realistically sized.

2. Mathematical Preliminaries

[7] We consider an ice mass in plug flow on a flat bed, where the horizontal velocity is vertically uniform for a given horizontal position. This can represent an ice-stream or a flow where the shear occurs in a very thin layer near the bed [*Fowler*, 1992]. The relation between the horizontal velocity and the basal shear stress can be represented by a sliding law. Membrane stresses and corresponding strain-rates are related by a non-linear viscous law, and horizontal force balance is represented by the commonly used equations due to *MacAyeal* [1989], or, for comparison, by the shallow ice approximation. Temperature is computed by solving a time-dependent advection-diffusion equation; the assumption of plug flow allows us to place all the dissipative heating, crucial to triggering instabilities, at the base of the ice. When the shallow ice approximation is used, an alternative horizontal motion constitutive equation, which represents internal deformation, is also used to test the influence of the initializing the ice-sheet. The numerical implementation is outlined in Appendix A. A square grid is used, and the parameters affecting the numerical solutions are the grid size $\Delta_x = \Delta_y$, the vertical discretization Δ_ζ and the time-step size Δ_t.

[8] Under the MSA, the governing equations for such an ice-mass are [*MacAyeal*, 1989]

$$2\frac{\partial H\tau_{xx}}{\partial x} + \frac{\partial H\tau_{yy}}{\partial x} + \frac{\partial H\tau_{xy}}{\partial y} - T_{tx} = \rho_i g H \partial_x H, \qquad (1a)$$

$$\frac{\partial H\tau_{xx}}{\partial y} + 2\frac{\partial H\tau_{yy}}{\partial y} + \frac{\partial H\tau_{xy}}{\partial x} - T_{ty} = \rho_i g H \partial_y H, \qquad (1b)$$

where τ is the deviatoric stress tensor, H is the thickness of ice, (x, y) are horizontal position, ρ_i, ρ_w are the densities of ice and water respectively and g the acceleration due to gravity. The vector $\mathbf{T}_t = (T_{tx}, T_{ty})$ is the basal tangential traction. Boundary conditions are zero tangential stress on the vertical planes defining the boundary, and a normal deviatoric stress τ_{nn}

$$\tau_{nn} = \gamma H/4, \qquad (2)$$

on these planes, where $\gamma \equiv (1-\rho_i/\rho_w)\ \rho_i g$, which is numerically equivalent to the force across a grounding line where no shelf is present. The surface elevation can evolve at the margin. These boundary conditions avoids difficulties associated with a moving grounding line, and numerical experiments showed that the exact boundary condition did not affect the results or conclusions of this paper, which depend upon processes occurring well upstream of the grounding-line. Where symmetry boundary conditions are prescribed this normal boundary condition is replaced by one setting the normal velocity to zero; the tangential condition is unchanged.

[9] The strain-rate tensor $\mathbf{e}$ is related to the stress tensor τ by the viscous relationship $\mathbf{e} = A\tau_{\mathrm{I}}^{n-1}\tau$, where A is the temperature-dependent rate factor, $\tau_{\mathrm{I}} = \frac{1}{2}\mathrm{trace}\ (\tau \cdot \tau)$ is the second invariant of the stress tensor and n is the Glen index. The evolution of thickness is given by $\partial_t H + \nabla \cdot (H\mathbf{u}) = a$, where t is time, $\mathbf{u}$ is the horizontal velocity vector, a is the surface accumulation rate and we assume negligible basal melting. Since the ice flows out of the boundary at all points, we allow ice thickness to vary freely at the margin under the membrane stress approximation.

[10] Since we assume that forward motion takes place at or near the bed, we represent this by a constitutive relationship for the tangential traction vector $\mathbf{T}_t$ and the velocity $\mathbf{u}$

$$\mathbf{T}_t = C|\mathbf{u}|^{\frac{1}{\ell}-1}\mathbf{u}, \qquad (3)$$

where ℓ is the index in a Weertman-type sliding law. We also carried out experiments with the shallow ice approximation, in which the membrane mechanical equation (1) is replaced by $-\mathbf{T}_t = \rho_i g H \nabla H$, i.e., the membrane terms are removed. This equation is now used with the constitutive relationship equation (3) to compute ice flow. In order to examine the effects of initial conditions on shallow ice solutions, in some experiments the constitutive relationship equation (3) is replaced by one which represents internal deformation occurring according to the shallow ice approximation as follows

$$\mathbf{T}_t = \left(\frac{n+2}{2AH}\right)^{\frac{1}{n}} |\overline{\mathbf{u}}|^{\frac{1}{n}-1}\overline{\mathbf{u}}, \qquad (4)$$

where $\overline{u}$ is the column-mean velocity, which gives the same results for isothermal case (A uniform) as the EISMINT I tests [*Huybrechts et al.*, 1996].

[11] Plug flow asymptotics [*Fowler*, 1992] justify mapping any heating in a basal shear layer onto a sliding heating term, and it is this term which drives the instability. This is the only dissipative term in the thermal equations,

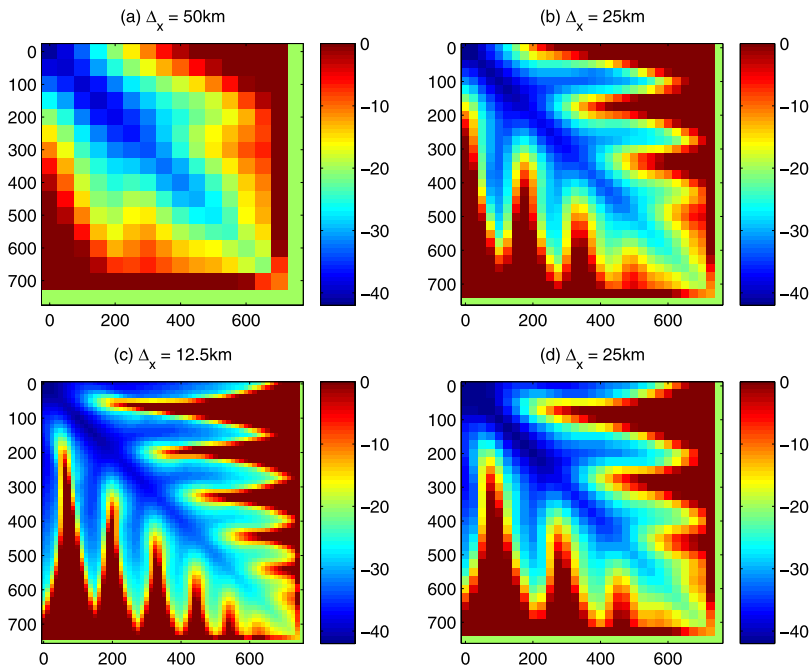

Figure 1. Steady basal temperature in °C using the shallow ice approximation, (a) 50 km; (b) 25 km; (c) 12.5 km grids, standard initialization (Figures 1a–1c); (d), 25 km grid, alternative initialization. *x*-coordinate horizontal on page. Note the dependence on grid size and initialization. The shallow ice approximation has been used in most thermoviscous calculations hitherto but gives multiple solutions.

which are written and solved in a ζ-coordinate system, where $\zeta = z/H$, i.e.,

$$\frac{\partial\theta}{\partial t} + \mathbf{u}\cdot\nabla_H\theta - \frac{a\zeta}{H}\frac{\partial\theta}{\partial\zeta} = \frac{k}{\rho c_s H^2}\frac{\partial^2\theta}{\partial\zeta^2}, \tag{5}$$

$$\theta(\mathbf{r}, \zeta = 1, t) = \theta^s(\mathbf{r}, s, t), \tag{6}$$

$$-\frac{k}{H}\frac{\partial\theta}{\partial\zeta}\bigg|_{\zeta=0} = G + \mathbf{T}_t\cdot\mathbf{u}, \tag{7}$$

where θ is the temperature, k is the thermal conductivity of ice, c_s is the specific heat capacity of ice, θ^s is the prescribed surface temperature, G is the geothermal heat flux and $\mathbf{T}_t$ is the basal tangential traction. The vertical advection term is the ζ-coordinate expression of continuity based on the divergence of horizontal velocity [*Hindmarsh*, 1999]. Internal heating $\mathbf{e}\cdot\tau$ is negligible because the flow is still shallow, and in any case such heating mostly occurs near the upper surface, because the ice is colder and stiffer there.

3. Numerical Experiments

3.1. Flow Domain and Specifications

[12] Similarly to the EISMINT [*Huybrechts et al.*, 1996] experiments, the flow domain is a square of sides 1500 km, and exploited symmetry, being solved on a quarter domain with sides of 750 km. The accumulation rate is uniformly 0.3 m.a^{-1}, and the indices $n = 3$, $\ell = 3$. The dependence of the rate factor on temperature was modelled by $A = A_0R(\theta)$.

[13] Here $R(\theta)$ incorporates a dual-Arhenius relationship

$$R(\theta) = c_1\exp\left(-\frac{E_1}{G_c\theta^2}\right) + c_2\exp\left(-\frac{E_2}{G_c\theta^2}\right) \tag{8}$$

proposed by *Hindmarsh and Le Meur* [2001], where $A_0 = 10^{-16}$ a^{-1}.Pa^{-3}, $(c_1, c_2) = (3.7\times10^6, 5.4\times10^{26})$, $(E_1, E_2) = (60, 140)$ kJ.mol^{-1} and G_c is the universal gas constant. By construction, R is 1 at the melting point of ice. The sliding coefficient C also has a temperature-dependence to simulate the dependence of shear on the temperature $C = C_0/R(\theta)$ with $C_0 = 4.47\times10^{-5}$.Pa.(m.a^{-1})$^{1/3}$. This value was chosen to produce a maximum elevation under isothermal conditions $R \equiv 1$ very similar to that given by the EISMINT I benchmark [*Huybrechts et al.*, 1996]. Also, $\rho_i = 910$ kg.m^{-3}, $g = 9.81$ m.s^{-2}, $k = 2$ W.m.K^{-1}, $c = 2008$ J.kg^{-1} have been used. The geothermal heat flux was set to 0.0438 W.m^{-2}, and surface temperature $\theta^s = -20 + 0.01HC$.

3.2. Shallow Ice Experiments

[14] Two initialization techniques were used. In the first one ("Standard initialization") the model was run in three stages: (i) the steady geometry was computed for an isothermal ice-sheet with $R \equiv 1$ using equation (4); (ii) the thermal field for this geometry, but with no thermo-viscous coupling was computed; (iii) the model was allowed to evolve with thermo-viscous coupling. Finally, (iv), the constitutive relationship equation (3) was used in place of equation (4), and the model run to steady state in thermo-viscously coupled mode. The second initialization ("Alternative initialization") technique consisted of the first three steps of the above, but using equation (3) throughout. These routes produced different results for the same grid size; the

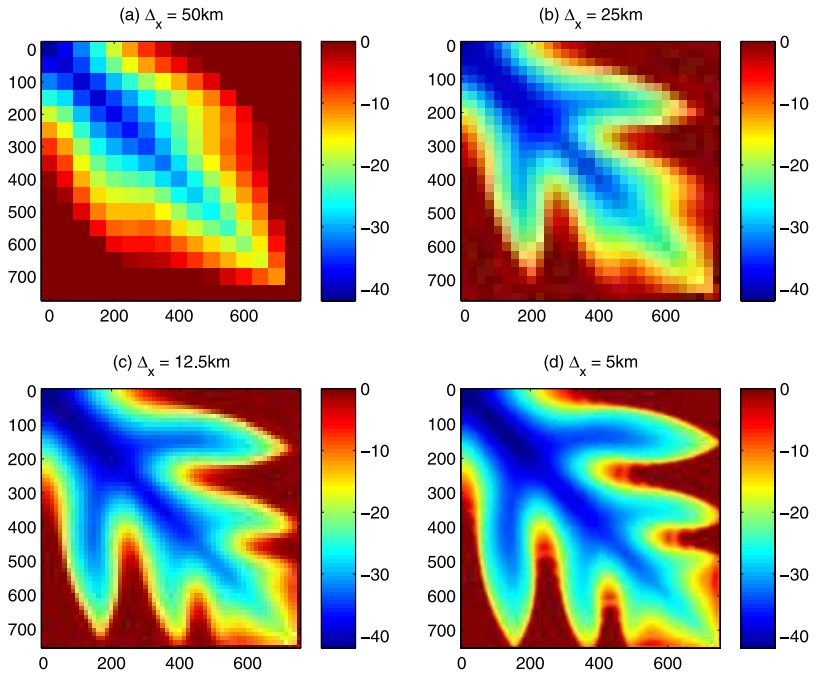

Figure 2. Steady basal temperature in °C with membrane stresses, (a) 50 km; (b) 25 km; (c) 12.5 km; (d) 5 km grids. Inclusion of membrane stresses generates a unique solution.

motivation for using the first, less intuitive route, is that it produced for one grid size stream patterns similar to those computed with membrane stresses. Computed steady basal temperatures for different grid sizes are shown in Figure 1. As in previous calculations [*Payne and Dongelmans*, 1997; *Payne et al.*, 2000] the uniform forcing results in a patterning of basal temperatures with warm parts corresponding to streams, arising from the ice-flux capture mechanism described by *Payne and Dongelmans* [1997]. However, the results show a clear dependence of stream geometry on grid size (Figures 1a–1c) and on initial conditions (Figure 1d).

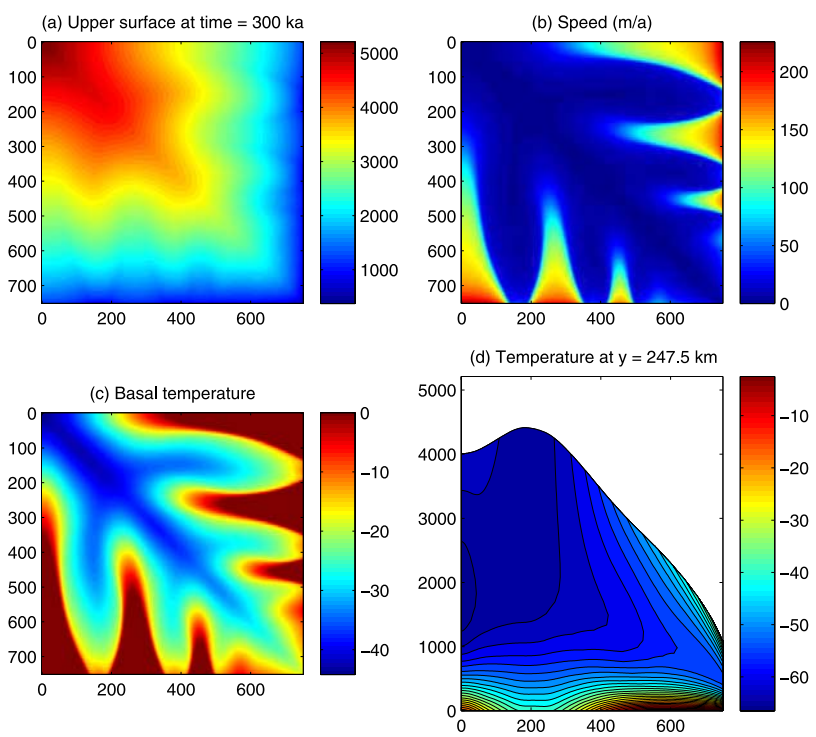

Figure 3. Steady temperatures and geometry with membrane stresses for 2.5 km grid, MSA, (a) thickness/elevation (m); (b) speed; (c) basal temperature (°C); (d) cross-section showing temperatures at indicated *y*-position.

3.3. Membrane Stresses

[15] Here we used the "Alternative Initialization", except that membrane stresses were incorporated for all three stages. Computed steady basal temperatures for different grid sizes are shown in Figure 2. Again, uniform forcing results in a patterning of basal temperatures, but the results now show consistent stream geometry with grid size apart from the very coarsest grid, with the transition between the warmer-based and colder-based flows sharpening as grid size is decreased. Figure 3 shows the finest resolution calculations (grid size 2.5 km) of basal temperature, surface elevation, speed and internal temperature. Figure 2d (5 km grid) shows some transverse patterning within the streams; this is not apparent in for the 2.5 km grid (Figure 3), and it is a consequence of the longer time-step used (125a); shortening the time-step for the 5 km grid to 50a removed these patterns. A further result, consistent with *Payne and Dongelmans* [1997], is that a plane flow (i.e., symmetry boundary condition on three sides) did not spontaneously produce streaming flow. Other experiments run by *Payne and Dongelmans* [1997] which investigated the effect of weak symmetry breaking, were not re-run.

4. Discussion

[16] These results show that on flat beds it is important to include horizontal stress gradients in the governing equations to produce consistent computations of stream geometry. The streams are between a few tens of kilometres to a hundred kilometres in width for these experiments, consistent with observed ice-streams, although a more exhaustive parameter study would be required to determine the general validity of this observation.

[17] As described above, *Payne and Dongelmans* [1997] proposed an ice-flux capture mechanism based on the way the SIA directs ice flow. Is this proposal still valid, given that the MSA is seen to be an essential component of robust prediction? Since one of the SIA calculations (Figure 1b) produces stream geometry comparable with the consistent calculations produced with the MSA (Figures 2 and 3), it seems that there is an initial case that this mechanism does operate; as *Hindmarsh* [2006a] argued, using the MSA stops shorter wavelength features being selected.

[18] *Hindmarsh* [2006b] estimated the membrane coupling length L (actually for the grounding line transition zone, but the same analysis applies here) to be given by $L = \left(2\frac{\left(A^{-1}u\right)^{\frac{1}{n}}}{\rho g \varepsilon}\right)^{\frac{n}{n+1}}$, where ε is a mean slope. For cold ice an upper surface value for A is $10^{-19} - 10^{-18}\mathrm{Pa}^{-3}.\mathrm{a}^{-1}$, and for the computed ice-sheets $\varepsilon \approx 0.005$. With a velocity of 100 $\mathrm{m.a}^{-1}$, the membrane coupling length is between 10 and 15 km. The computed ice-streams are therefore significantly wider than the membrane coupling length, which is further support that the ice-flux capture mechanism is qualitatively correct.

[19] It may emerge that in areas where the flow is channelled by basal topography, incorporation of membrane stresses is not necessary to produce reliable computation of stream location. Further work should investigate this issue, looking particularly at whether certain wavelengths in basal topography are more able to control stream location. Other issues include the investigation of how weak symmetry breaking can be before streams stop spontaneously appearing, as well as the generation of surges within the streams. More generally, since one does not know a priori where streams will appear, the simplest course would appear to be to solve for membrane stresses everywhere, as has been the procedure in this paper.

Appendix A: Numerical Implementation

[20] The momentum balance equations are solved using a conservative finite difference method on a staggered grid. Ice thicknesses are defined on the nodes, and x- and y-direction velocities on the same staggered grids as used in the shallow ice approximation [e.g., *Hindmarsh and Payne*, 1996], which are also the locations of the solution points for the x- and y-momentum balance equations. Normal stresses τ_{xx}, τ_{yy} are defined on the nodes, while shear stress τ_{xy} is defined on the grid centres. The continuity equation is solved on the thickness points. The equations are solved semi-implicitly with a super-implicit weighting of $\omega = 3$; this guarantees numerical stability for the membrane stress case as well as the SIA case [*Hindmarsh*, 2001].

References

Bamber, J. L., D. G. Vaughan, and I. R. Joughin (2001), Widespread complex flow in the interior of the Antarctic ice sheet, *Science*, *287*, 1248–1250.

Blatter, H. (1995), Velocity and stress-fields in grounded glaciers-A simple algorithm for including deviatoric stress gradients, *J Glaciol.*, *41*, 333–344.

Bueler, E., J. Brown, and C. Lingle (2007), Exact solutions to the thermo-mechanically coupled shallow ice approximation: Effective tools for verification, *J. Glaciol.*, *53*, 499–516.

Clark, C. D. (1993), Mega-scale glacial lineations and cross-cutting ice-flow landforms, *Earth Surf. Processes Landforms*, *18*, 1–29.

Fowler, A. C. (1992), Modelling ice sheet dynamics, *Geophys. Astrophys. Fluid Dyn.*, *63*, 29–65.

Fowler, A. C., and C. Johnson (1996), Ice sheet surging and ice stream formation, *Ann. Glaciol.*, *23*, 68–73.

Hindmarsh, R. C. A. (1999), On the numerical computation of temperature in an ice-sheet, *J. Glaciol.*, *45*, 568–574.

Hindmarsh, R. C. A. (2001), Notes on basic glaciological computational methods and algorithms, in *Continuum Mechanics and Applications in Geophysics and the Environment*, edited by B. Straughan et al., pp. 222–249, Springer, Berlin.

Hindmarsh, R. C. A. (2004), Thermoviscous stability of ice-sheet flows, *J. Fluid. Mech.*, *502*, 17–40.

Hindmarsh, R. C. A. (2006a), Stress gradient damping of thermoviscous ice flow instabilities, *J. Geophys. Res.*, *111*, B12409, doi:10.1029/2005JB004019.

Hindmarsh, R. C. A. (2006b), The role of membrane-like stresses in determining the stability and sensitivity of the Antarctic ice-sheets: Back-pressure and grounding line motion, *Philos. Trans. R. Soc., Ser. A*, *364*, 1733–1767, doi:10.1098/rsta.2006.1797.

Hindmarsh, R. C. A., and E. Le Meur (2001), Dynamical processes involved in the retreat of marine ice sheets, *J. Glaciol.*, *47*, 271–282.

Hindmarsh, R. C. A., and A. J. Payne (1996), Time-step limits for stable solutions of the ice-sheet equation, *Ann. Glaciol.*, *23*, 74–85.

Hulbe, C. L., and D. R. MacAyeal (1999), A new thermodynamical numerical model of coupled ice sheet, ice stream, and ice shelf flow, *J. Geophys. Res.*, *104*, 25,349–25,366.

Huybrechts, P., and T. Payne (1996), The EISMINT benchmarks for testing ice-sheet models, *Ann. Glaciol.*, *23*, 1–12.

MacAyeal, D. R. (1989), Large-scale ice flow over a viscous basal sediment: Theory and application to ice stream B, Antarctica, *J. Geophys. Res.*, *94*, 4071–4088.

MacAyeal, D. R. (1993), A low-order model of growth/purge oscillations of the Laurentide ice-sheet, *Paleoceanography*, *8*, 767–773.

Marshall, S. J., and G. K. C. Clarke (1997), A continuum mixture model of ice stream thermomechanics in the Laurentide Ice Sheet: 2. Application to the Hudson Strait Ice Stream, *J. Geophys. Res.*, *102*, 20,615–20,637.

Payne, A. J. (1995), Limit cycles in the thermal regime of ice sheets, *J. Geophys. Res.*, *100*, 4249–4263.

Payne, A. J., and P. Dongelmans (1997), Self-organization in the thermo-mechanical flow of ice-sheets, *J. Geophys. Res.*, *102*, 12,219–12,233.

Payne, A. J., et al. (2000), Results from the EISMINT intercomparison: The effects of thermo-mechanical coupling, *J. Glaciol.*, *46*, 227–238.

Saito, F., A. Abe-Ouchi, and H. Blatter (2006), European Ice Sheet Modelling Initiative (EISMINT) model intercomparison experiments with first-order mechanics, *J. Geophys. Res.*, *111*, F02012, doi:10.1029/2004JF000273.

Sayag, R., and E. Tziperman (2008), Spontaneous generation of pure ice streams via flow instability: Role of longitudinal shear stresses and subglacial till, *J. Geophys. Res.*, *113*, B05411, doi:10.1029/2007JB005228.

Vaughan, D. G., H. F. J. Corr, F. Ferraccioli, N. Frearson, A. O'Hare, D. Mach, J. W. Holt, D. D. Blankenship, D. L. Morse, and D. A. Young (2006), New boundary conditions for the West Antarctic ice sheet: Subglacial topography beneath Pine Island Glacier, *Geophys. Res. Lett.*, *33*, L09501, doi:10.1029/2005GL025588.

R. C. A. Hindmarsh, Physical Sciences Division, British Antarctic Survey, Natural Environment Research Council, High Cross, Madingley Road, Cambridge CB3 0ET, UK. (rcah@bas.ac.uk)